© 2015. Published by The Company of Biologists Ltd | The Journal of Experimental Biology (2015) 218, 2573-2584 doi:10.1242/jeb.119438

RESEARCH ARTICLE

XROMM analysis of tooth occlusion and temporomandibular joint kinematics during feeding in juvenile miniature pigs

Rachel A. Menegaz[1,*], David B. Baier[2], Keith A. Metzger[3], Susan W. Herring[4] and Elizabeth L. Brainerd[5]

ABSTRACT

Like humans, domestic pigs are omnivorous and thus are a common model for human masticatory function. Prior attempts to characterize food–tooth interactions and jaw movements associated with mastication have been limited to aspects of the oral apparatus that are visible externally (with videography) and/or to 2D movements of oral structures (with monoplanar videofluoroscopy). We used XROMM, a 3D technique that combines CT-based morphology with biplanar videofluoroscopy, to quantify mandibular kinematics, tooth occlusion and mandibular condylar displacements within the temporomandibular joint (TMJ) during feeding. We observed that the pig TMJ moved detectably in only three of six possible degrees of freedom during mastication: two rotations, pitch and yaw; and one translation, protraction–retraction. Asymmetrical yaw around a dorsoventral axis produced the observed alternating left–right chewing cycles responsible for food reduction. Furthermore, the relative motions of the upper and lower premolars contained a substantial mesiodistal component in addition to the buccolingual component, resulting in an oblique (rather than a strictly transverse) power stroke. This research demonstrates the capacity of XROMM to explore the kinematic underpinnings of key masticatory movements, such as the occlusal power stroke, by integrating tooth, joint and rigid body jaw movements. XROMM also allowed us to test kinematic hypotheses based on skeletal anatomy with actual kinematics observed during naturalistic feeding behaviors. We observed that the soft tissue structures of the TMJ appear to play a significant role in limiting the range of motion of a joint, and thus analyses based solely on osseous morphology may over-estimate joint mobility.

KEY WORDS: Mastication, TMJ, Jaw kinematics, Power stroke, Tooth cusp

INTRODUCTION

Domestic pigs and their wild relatives are true omnivores with a diverse diet. Feral pigs in North America are known to consume a wide range of vegetation, including grasses, roots, cacti, nuts and agricultural crops, as well as invertebrates, small vertebrates and indigestible debris (Graves, 1984; Taylor, 1999). Because of similarities in diet, pigs are convergent in their craniodental morphology with other omnivores, such as ursids and hominin primates (Scheman, 1967; Bodegom, 1969; Hatley and Kappelman, 1980). These morphologies, specifically bunodont molars with thick enamel and mobile temporomandibular joints, are thought to facilitate the transverse grinding and crushing motions used to process a wide range of brittle or gritty food items (Herring, 1976, 1985; Janis and Fortelius, 1988).

The bunodont molars of pigs are distinct from those of other omnivores because of the formation of two transverse enamel ridges that join the buccal and lingual cusps (Herring and Scapino, 1973; Herring, 1976). During the occlusal power stroke, transverse movements of the mandible produce grinding between the ridges and valleys of opposing teeth, and shear between the vertical facets of opposing ridges (Herring, 1976). Furthermore, food is often present bilaterally in the mouth of the pig during mastication (Herring, 1976; Sun et al., 2002). This produces an unusual pattern of alternating chewing, in which, from external views, the lower incisors appear to translate laterally across the midline towards one side and then back across the midline towards the other side in an alternating pattern of sequential chews (Herring and Scapino, 1973; Herring, 1976; Langenbach et al., 2002).

In pigs, as in many herbivorous and omnivorous mammals, transverse grinding motions result primarily from the rotation of the jaw around a dorsoventrally oriented axis (‘yaw’) located between the mandibular condyles (Smith and Savage, 1959; Herring and Scapino, 1973). Yaw rotations are powered by muscle triplets (*sensu* Weijs, 1994), which act to protract one side of the mandible while simultaneously retracting the opposite side (Herring and Scapino, 1973; Weijs, 1994). In humans, mediolateral translations of the mandibular condyles have been hypothesized (Bennett, 1908), but largely disproven (Landa, 1958a,b).

There are few skeletal or dental structures to limit chewing movements in pigs (Herring, 1985, 1993). The transverse ridges of the molars form inclined planes which may contribute to the directionality of the power stroke, but these ridges and their associated cusps are low and become worn rapidly in the presence of an abrasive diet (Janis and Fortelius, 1988; Herring, 1993). Likewise, the temporomandibular joint (TMJ) of domestic pigs has few osseous structures to restrict movements. As in humans, the mandibular condyle of the pig articulates against the articular eminence of the temporal bone. The strongly curved surface of the articular eminence permits anterior movements of the condyle. Posteriorly, the postglenoid wall is absent in pigs and the space is filled with a fibrous-fatty retrodiscal pad, which is flexible enough to allow slight retraction of the mandibular condyle (Sindelar and Herring, 2005). Thus, based on both bony and soft tissue morphology, we anticipate a high degree of anteroposterior mobility for the mandibular condyles in the miniature pig.

Similarly, the mediolateral movements of the mandibular condyle appear to be relatively unconstrained by osseous structures. A flange of the zygomatic arch projects inferiorly to the level of the condyle and may limit lateral movements of the condyle (Herring et al., 2002; Sun et al., 2002), while the medial aspect of the articular process is

[1]Department of Biomedical and Applied Sciences, Indiana University School of Dentistry, Indianapolis, IN 46202, USA. [2]Department of Biology, Providence College, Providence, RI 02918, USA. [3]Department of Anatomy and Structural Biology, Albert Einstein College of Medicine, Yeshiva University, Bronx, NY 10461. [4]Department of Orthodontics, University of Washington, Seattle, WA 98195, USA. [5]Department of Ecology and Evolutionary Biology, Brown University, Providence, RI 02912, USA.

*Author for correspondence (rmenegaz@iu.edu)

Received 21 January 2015; Accepted 3 June 2015

The Journal of Experimental Biology (2015) 218, 2573-2584 doi:10.1242/jeb.119438

List of abbreviations

ACS	anatomical coordinate system
BS	balancing side
dP	deciduous premolar
JCS	joint coordinate system
TMJ	temporomandibular joint
WS	working side
XROMM	X-ray reconstruction of moving morphology

bounded by the auditory bulla and mastoid and paracondylar processes. However, even though we would predict some degree of transverse mobility of the mandibular condyle based on hard tissues, soft tissues of the joint capsule may play a role in limiting mediolateral movements, as the medial and lateral ligaments of the capsule are well developed (Herring et al., 2002; Sun et al., 2002). In comparison to the human capsule, the medial ligament in pigs is particularly well reinforced and may restrict lateral deviations of the mandibular condyle (Herring et al., 2002; Sun et al., 2002). Therefore, based on hard-tissue morphology, we predict a highly mobile TMJ, but based on soft-tissue morphology, we predict the mediolateral translations of the condyles to be very small or absent.

In this study, we tested these predictions regarding mandibular condyle mobility and we investigated the occlusal movements responsible for food reduction in the context of motions occurring at the more posterior TMJ. Historically, *in vivo* motions of the posterior mandible, including the cheek teeth and the TMJ, have been difficult to visualize during feeding because of the overlying tissues. Alternative approaches have included using light video to track externally visible structures, such as the snout/chin and incisors, to then infer mandible and/or molar motions, and using uniplanar fluoroscopy to track the two-dimensional movements of oral structures. Here, we used XROMM (X-ray reconstruction of moving morphology), a technique that combines CT-based morphology with biplanar videofluoroscopy (Brainerd et al., 2010), to directly measure 3D mandibular kinematics in miniature pigs (*Sus scrofa*) during feeding. We describe the kinematics of chewing, food gathering and nut crushing in order to encompass the full range of feeding behaviors used by the pig. Our aims were as follows: (1) to measure the six-degree-of-freedom (three translations and three rotations) motions of the mandible during feeding; (2) to measure tooth displacements during mastication and to examine the relative movement of opposing teeth during occlusion; and (3) to measure condylar displacements during feeding. In doing so, our goal was to describe the process of food reduction during pig feeding in the context of mandibular movements that link the actions of the teeth with the actions of the temporomandibular joint.

RESULTS

Kinematic variables in this study are expressed relative to the cranium as biologically relevant translations, rotations and displacements (Tables 1, 2). Our mandibular joint coordinate system (JCS) describes the movements of the mandible relative to the cranium through two anatomical coordinate systems (ACSs), one attached to the cranium and the other to the mandible (Figs 1, 2, Table 1). Displacements of anatomical landmarks on the teeth and mandibular condyles were described relative to a cranial ACS (Figs 1, 2, Table 1). Precision thresholds were applied to all kinematic variables in order to distinguish measurable, repeatable motions from accumulated noise within the XROMM workflow (Table 3).

Chewing kinematics

During mastication, mandibular translations were largely propalinal along an anteroposterior axis (T_x) (Fig. 2). Individuals in this study were observed to retract the jaw a mean 5.38±1.41 mm between the opening phase and the occlusal phase of a chew (N=29 chews). In two of the three individuals, translations along the other axes (T_y and T_z) rarely exceeded their precision thresholds (Table 3). This was indicative of a lack of significant dorsoventral or lateral translation of the jaw during mastication (but see 'Interindividual variation', below).

The major rotational movement occurring during mastication was pitch of the mandible around the transverse axis (R_z), corresponding to jaw depression and elevation (Fig. 2). Individuals in this study were observed to close the jaw a mean 13.67±1.93 deg between the opening phase and the occlusal phase of a chew (N=32 chews). Mandibular pitch (R_z) and propalinal translation (T_x) were closely linked during mastication (Fig. 2), such that 1 deg of jaw depression was associated with 0.37–0.45 mm of jaw protraction during the opening phase of a chew (Table 4). Yaw of the mandible around a dorsoventral axis (R_y) resulted in displacements along the post-canine tooth row and at the mandibular condyles (described below). No significant movement was observed in the roll of mandible about an anteroposterior axis (R_x).

All individuals in this study exhibited left/right alternating chewing, a behavior typical of the pig (Herring and Scapino, 1973; Herring, 1976; Langenbach et al., 2002) (Fig. 2). Alternating chewing sequences were marked by reversal in the direction of mandibular yaw (R_y) during the occlusal phase with each cycle (Fig. 3). The side toward which mandibular yaw was directed during the jaw-opening phase is the working side (WS), while the contralateral side is the balancing side (BS). Kinematic measures

Table 1. Kinematic variables described relative to the cranium

Element	Data source[1]	Abbreviation	Description[2]
Mandible	JCS	T_x	Anterior translation of the jaw (protraction)
		T_y	Dorsal translation of the jaw
		T_z	Lateral translation of the jaw to the right
		R_x	Roll of the jaw towards the left
		R_y	Yaw of the jaw to the left
		R_z	Pitch of the jaw dorsad (elevation/closing)
Mandibular deciduous premolar 4	ACS	Od_x	Mesial displacement
		Od_y	Dorsal displacement
		Od_z	Buccal/lingual displacement to the right
Mandibular condyles	ACS	Cd_x	Anterior displacement
		Cd_y	Dorsal displacement
		Cd_z	Lateral displacement to the right

[1]Type of axis system used to export data from XROMM (X-ray reconstruction of moving morphology) animations: JCS, joint coordinate system; ACS, anatomical coordinate system.
[2]Polarity is determined by ACS orientation and the right-hand rule. Motion in the positive direction is indicated here.

The Journal of Experimental Biology (2015) 218, 2573-2584 doi:10.1242/jeb.119438

Table 2. Definitions of measurements taken from kinematic variables in this study

Measurement	Abbreviation	Definition
Jaw retraction	ΔT_x	Difference in T_x between maximum protrusion and maximum retrusion during a chew/food-gathering movement
Jaw closing	ΔR_z	Difference in R_z between maximum depression and maximum elevation during a chew/food-gathering movement
Occlusal displacement (mesiodistal)	ΔOd_x	Difference in Od_x between the beginning and the end of the occlusal phase
Occlusal displacement (buccolingual)	ΔOd_z	Difference in Od_z between the beginning and the end of the occlusal phase
Condylar retraction	ΔCd_x	Difference in Cd_x between the beginning and the end of the closing or occlusal phase of a chew

of jaw movement during chewing were taken from alternating chewing sequences (Tables 1, 2). Two of the three individuals also exhibited non-alternating chewing, during which chews only occurred on a single side. Non-alternating chewing was observed only in small sequences (<4 chews), either isolated by food-gathering events or leading into a longer alternating chewing sequence (as in Fig. 3).

Occlusal displacements

Bilateral occlusion was observed during mastication in the miniature pig. During the occlusal phase of a right-sided chew, the ipsilateral (right) mandibular dP4 (deciduous premolar 4) underwent lingual (Od_z) and mesial (Od_x) displacements relative to the cranial ACS (Fig. 4). Thus, during the power stroke, the motions of the WS mandibular corpus were directed both medially and anteriorly. Displacements along the mesiodistal axis (Od_x) were approximately 1/3 as large as those along the buccolingual axis (Od_z) (Table 5). When combined with the lingual displacements (Od_z) that occurred during occlusion, the mesial displacements of the mandibular dP4 (Od_x) produced an oblique, rather than strictly transverse, power stroke. These occlusal displacements were associated with mandibular yaw (R_y) towards the BS during the occlusal phase of the chew (Fig. 4D).

Food processing also may occur along the BS tooth row. During the occlusal phase of a left-sided chew, the contralateral (right) mandibular dP4 underwent buccal (Od_z) and distal (Od_x) displacements relative to the cranial ACS (Fig. 4C). The magnitudes of displacements for the right mandibular dP4 along the mesiodistal (Od_x) and buccolingual (Od_z) axes were comparable between ipsilateral and contralateral chews (Table 5).

Condylar displacements

Displacements of the mandibular condyles along an anteroposterior axis during mastication resulted primarily from rotational depression and elevation of the jaw (R_z). Differences in the magnitude of these anteroposterior displacements (Cd_x) between the ipsilateral/WS and the contralateral/BS condyles were associated with the direction of mandibular yaw (R_y) (Fig. 5). During the opening phase, depression of the jaw (R_z) coincided with yaw of the mandible (R_y) towards the WS and greater protraction (Cd_x) of the contralateral/BS mandibular condyle than its ipsilateral/WS counterpart. Absolute protraction distance (the difference in Cd_x between the beginning and end of the phase) did not differ significantly between the condyles, but rather the contralateral/BS condyle was more protracted relative to its ipsilateral/WS counterpart throughout the entirety of the opening phase. The initial WS-directed yaw of the mandible was then followed by BS-directed yaw during the closing and occlusal phases. This secondary BS-directed mandibular yaw produced absolute condylar retraction measurements that were similar between sides during the closing phase, but significantly different ($P<0.01$) during the occlusal phase when the contralateral/BS condyle was retracted while the ipsilateral/WS condyle was protracted (Table 6). This difference in ipsilateral/WS versus contralateral/BS condylar movement then influenced the starting position of the condyles during the opening phase of the subsequent chew. Condylar displacements along the other axes (Cd_y and Cd_z) rarely exceeded their precision thresholds, indicating no significant dorsoventral or mediolateral displacements of the condyle during mastication. This is consistent with the absence of significant mandibular translations along these axes, and suggests that rigid body rotations are predominantly responsible for dorsoventral and mediolateral movements of the mandible.

Interindividual variation

One individual, Sus D, exhibited distinct differences in rigid body kinematics during mastication as compared with the other two individuals. Sus D produced conservative chews, with the smallest magnitudes of jaw depression–elevation and protraction–retraction. During the opening phase, only Sus D failed to protract the anterior margin of the mandibular condyles past the anterior border of the mandibular fossa, likely as a result of the small magnitude of jaw depression produced. Furthermore, jaw translation along a dorsoventral axis (T_y) that exceeded precision thresholds was only observed in Sus D. A mean of 1.05±0.19 mm of dorsal jaw translation was recorded for Sus D during the closing and occlusal phases (N=18 chews). Sus D also differed from the other individuals by displaying significantly greater ($P\leq0.01$) retraction of the BS condyle during both the closing and the occlusal phases (Table 6). While the origin of these kinematic differences is unknown, CT scans suggest that Sus D possessed an atypical TMJ and potentially may have had a displacement of the TMJ disc (supplementary material Fig. S1).

Food-gathering kinematics

Rigid body kinematics of the mandible were quantified for the food-gathering behavior exhibited by all individuals. During food gathering, jaw motion was limited to propalinal translations (T_x) and rotations that produce depression and elevation (R_z) (Fig. 6). Furthermore, during food gathering, the jaw was held in a protracted posture with a limited range of jaw opening (Fig. 7). During the opening phase of food gathering, 1 deg of jaw depression was associated with 0.31–0.42 mm of jaw protraction (Table 4). Reduced measures of jaw retraction (mean 2.85±1.36 mm, N=44 chews) and jaw closing (mean 5.85±3.05 deg, N=46 chews) were observed during food gathering, and the jaw was never retracted or closed to the full extent observed during chewing (Fig. 7). In addition to the rigid body motions of the mandible, motions of the tongue and snout contributed substantially to the behaviors exhibited during food gathering. The tongue protracted as the mandible was depressed, food was collected on the surface of the

The Journal of Experimental Biology (2015) 218, 2573-2584 doi:10.1242/jeb.119438

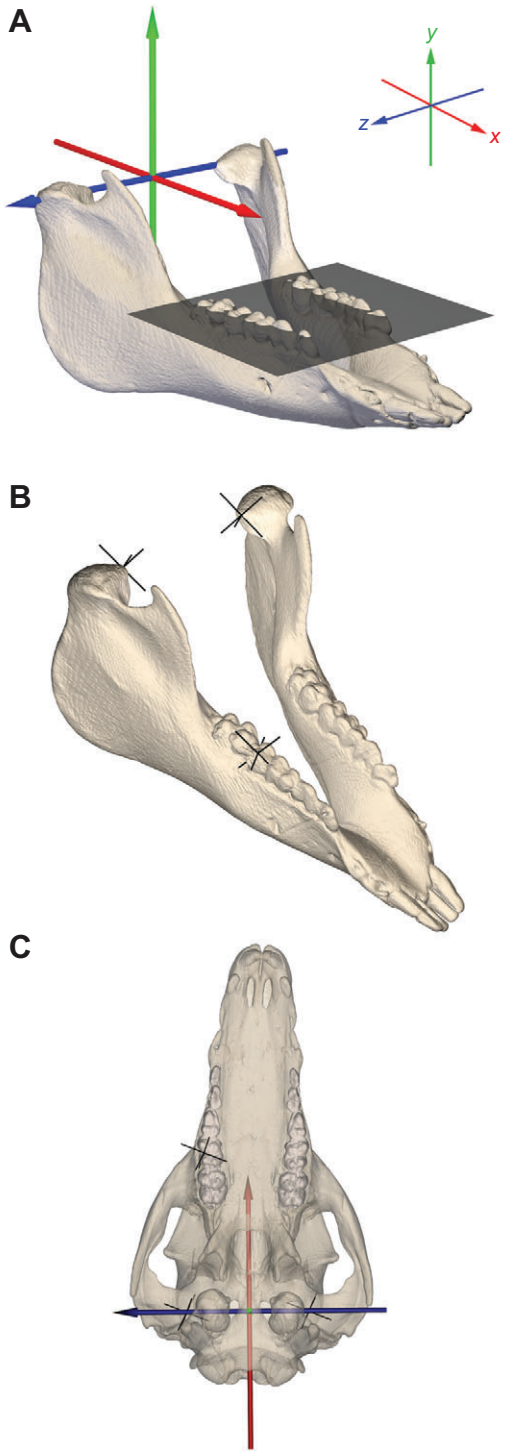

Fig. 1. The mandibular anatomical coordinate system (ACS) and anatomical locators used in this study. (A) Mandibular ACS with the *x*-axis aligned parallel to the occlusal plane (gray). (B) Anatomical locators (black cross-hairs) attached to the mandible: the right mandibular deciduous premolar 4 (dP4) and the medial-most points on the mandibular condyles (left and right). (C) Inferior view of the cranium showing the mandibular locators relative to the neutral position ACS attached to the cranium (*y*-axis is oriented superiorly, projecting away from the viewer).

tongue, and then the tongue retracted as the mandible was elevated. These soft tissue motions were not quantified here, but can be observed in the publicly accessible X-ray videos used in this study (see Minipig Feeding Study at www.xmaportal.org).

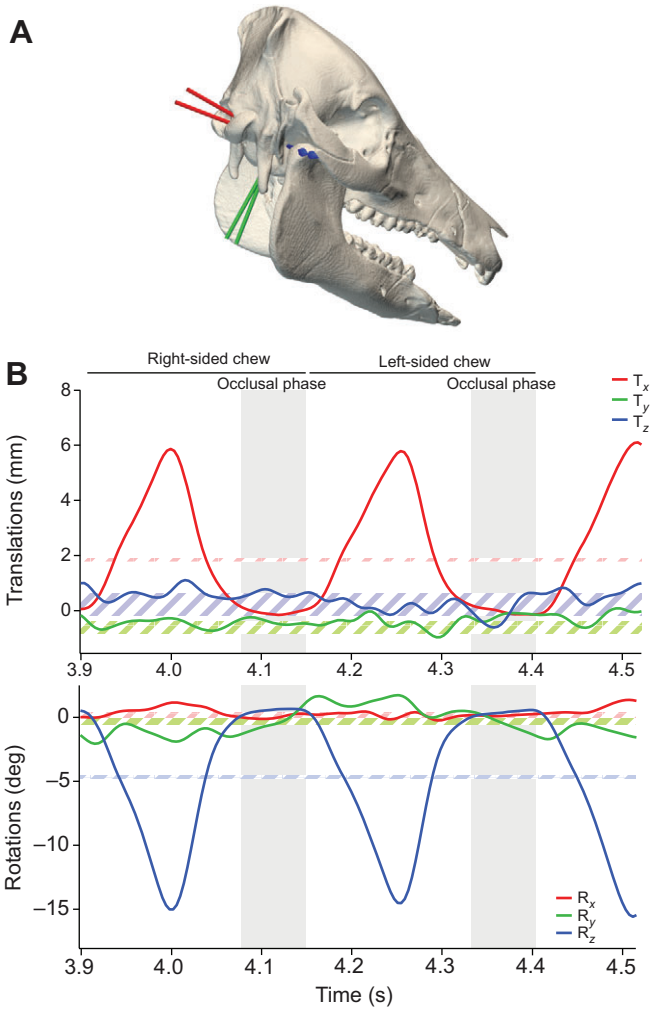

Fig. 2. Alternating chewing in the miniature pig. (A) The joint coordinate system (JCS) used in this study to describe motions of the mandible relative to the cranium. The output from the JCS is the six-degree-of-freedom motion between the two sets of axes (one attached to the mandible, the other to the cranium). (B) An alternating chewing cycle, here in pig Sus A, consists of a right-sided and then a left-sided chew. The opening phase of a subsequent right-sided chew is also shown. When the right side is the working side (WS), the mandible yaws toward the left during occlusion (increasing R_y); when the left side is the WS, the mandible yaws toward the right (decreasing R_y). Horizontal hatched bars show the precision thresholds for each degree of freedom.

Nut-crushing kinematics

During feeding trials in which two individuals were presented with unshelled nuts, the following stages of movement were observed: first, the nut was transported and positioned along the tooth row (transport stage); next, a slow series of cracking attempts was made, repositioning the nut as necessary (cracking stage); finally, after the nut was cracked, subsequent chews resulted in a progressive crushing of the nut as it was reduced to smaller particles (reduction stage).

During the nut-cracking stage, jaw motion was largely restricted to propalinal translations (T_x) and elevation/depression (R_z) (Fig. 8). Next, during the reduction stage, jaw motion became more similar to the chewing kinematics observed with pellets. Cyclical, non-alternating chewing with opening-phase mandibular yaw (R_y) towards the WS was present at this point. Furthermore, during the last stage, the particle size of the food item initially limited jaw

The Journal of Experimental Biology (2015) 218, 2573-2584 doi:10.1242/jeb.119438

Table 3. Precision threshold values for the kinematic variables used in this study

Coordinate system	Kinematic variables					
JCS	T_x	T_y	T_z	R_x	R_y	R_z
	0.06 mm	0.26 mm	0.44 mm	0.26 deg	0.21 deg	0.13 deg
ACS	Od_x	Od_y	Od_z	Cd_x	Cd_y	Cd_z
	0.13 mm	0.14 mm	0.30 mm	0.14 mm	0.28 mm	0.55 mm

retraction and closing. This resulted in a series of chews with a characteristic step-wise reduction in the magnitude of jaw retraction (T_x) and closing (R_z) patterns (e.g. 0.7–1.5 s; Fig. 8).

DISCUSSION

During mammalian mastication, opposing teeth must be brought into close proximity in order to produce the occlusal forces that will reduce food particle size. Food–tooth interactions occur relatively anteriorly along the jaw but are driven by motions occurring at the more posterior TMJ. In miniature pigs, mastication is characterized by an alternating transverse grinding of the post-canine dentition (Fig. 3) (Herring and Scapino, 1973; Herring, 1976; Langenbach et al., 2002). The osseous morphology of the TMJ in pigs indicates a fair degree of mobility and the capacity for both translational and rotational movements. Conversely, the arrangement of soft tissues (e.g. capsular ligaments) surrounding the TMJ suggests a restriction of transverse condylar translations, particularly relative to anteroposterior translations (Herring et al., 2002; Sun et al., 2002). We observed that the lateral grinding movements of pig mastication were produced by jaw rotations around a vertical axis accompanied by anteroposterior translations. We did not observe any contribution to the transverse chewing cycle from mediolateral deviations of the mandibular condyle, consistent with the kinematic predictions derived from the skeletal and particularly the soft tissue morphology of the TMJ. The observation that transverse grinding motions are produced by mandibular yaw is also consistent with previous studies of jaw motion and motor patterns in mammals, particularly in many artiodactyls and anthropoid primates (Smith and Savage, 1959; Herring and Scapino, 1973; Weijs, 1994; Hylander et al., 2005; Williams et al., 2007).

We found that, during occlusion, the buccolingual (transverse) translation of the premolar chewing surfaces primarily resulted from yaw rotations of the mandible (Fig. 4). We also noted that, during occlusion, the WS mandibular motions were directed both medially and anteriorly, resulting in an oblique rather than purely transverse power stroke (see Herring, 1993). Mesiodistal (anteroposterior) tooth translation was considerable during the power stroke, about 1/3 as large as buccolingual motions, but still likely to contribute toward food breakdown (Fig. 4). This oblique power stroke was observed despite the transverse enamel ridges of the deciduous premolars in the juvenile pig, suggesting that the presence of food material may prevent the complete intermeshing of occluding teeth (Herring and Scapino, 1973). It is also possible that this oblique power stroke is specific to juvenile pigs, as musculoskeletal growth and the changing orientation of masticatory muscles may produce a reorientation of the power stroke across ontogeny (Obrez, 1996).

Table 4. Results of least-square regressions of opening-phase jaw protraction against jaw depression

	Chewing		Food gathering	
	Slope	*y*-intercept	Slope	*y*-intercept
Sus A	−0.45	0.41	−0.36	2.49
(*N*=9 chews/12 FG cycles)	(0.01)	(0.07)	(0.02)	(0.13)
Sus B	−0.45	0.41	−0.42	1.71
(*N*=9 chews/10 FG cycles)	(0.01)	(0.04)	(0.03)	(0.21)
Sus D	−0.37	0.09	−0.31	1.44
(*N*=18 chews/11 FG cycles)	(0.00)	(0.02)	(0.03)	(0.17)
All individuals	−0.44	0.16	−0.48	1.17
(*N*= 36 chews/32 FG cycles)	(0.00)	(0.03)	(0.02)	(0.12)

Absolute values of slopes (s.d.) indicate the jaw protraction (T_x, mm) produced by 1 deg of jaw depression (R_z). FG, food gathering.

The isognathous jaws of miniature pigs facilitate bilateral occlusion during mastication (Herring and Scapino, 1973; Herring et al., 2001). We observed bilateral occlusion with comparable magnitudes of ipsilateral and contralateral tooth displacement (Fig. 4, Table 5), suggesting that both sides of the dentition may contribute to food breakdown. However, as we did not add radiopaque material to the food, it remains unclear whether the bolus was transported between sides during alternating chewing or whether boluses were present bilaterally. Yaw of the mandible was associated with the observed asymmetry in mandibular condyle translations during the occlusal phase of chews. Condylar retraction was largely produced by the rotational movements of jaw elevation during the closing phase, but we found that differences in the direction of condylar translation (protraction versus retraction) were related to the directional yaw of the mandible towards the BS during occlusion (Fig. 5). Because of the kinematics of mandibular yaw, the contralateral/BS condyle will always be relatively protracted compared with the ipsilateral/WS condyle during the opening and closing phases. These relative positions then switch during the occlusal phase, when the contralateral/BS condyle experiences retraction and the ipsilateral/WS condyle experiences protraction. The differential translations of the contralateral/BS condyle affect soft tissue deformation and strain at the TMJ (Liu and Herring, 2001; Sindelar and Herring, 2005).

Notably, we did not observe a tight mechanical coupling of rotations (e.g. jaw depression) and translations (e.g. jaw protraction) across all feeding behaviors. Jaw posture in pigs was flexible and changed between feeding behaviors. During food gathering, for example, the jaw was held in a more protracted posture with a more limited range of jaw depression and elevation as compared with the posture observed during mastication (Fig. 7).

During the consumption of hard objects, such as unshelled nuts, distinct differences existed between the kinematics of cracking the nut's shell (cracking phase) and the reduction of the nut material into smaller particle sizes (reduction phase). The cracking stage was characterized by limited jaw motions, with only propalinal translations and pitch rotations (Fig. 8). In the subsequent reduction stage, jaw motions were progressively more similar to those observed during the mastication of chow as a result of the presence of yaw rotations. However, only non-alternating chewing was observed during the consumption of nuts. The reduction of nut particle size with each chew resulted in a characteristic step-wise pattern of jaw retraction (T_x) and closing (R_z) (Fig. 8).

XROMM precision

The strength of the XROMM technology is evidenced both in its unique ability to visualize *in vivo* 3D skeletal kinematics and in its

The Journal of Experimental Biology (2015) 218, 2573-2584 doi:10.1242/jeb.119438

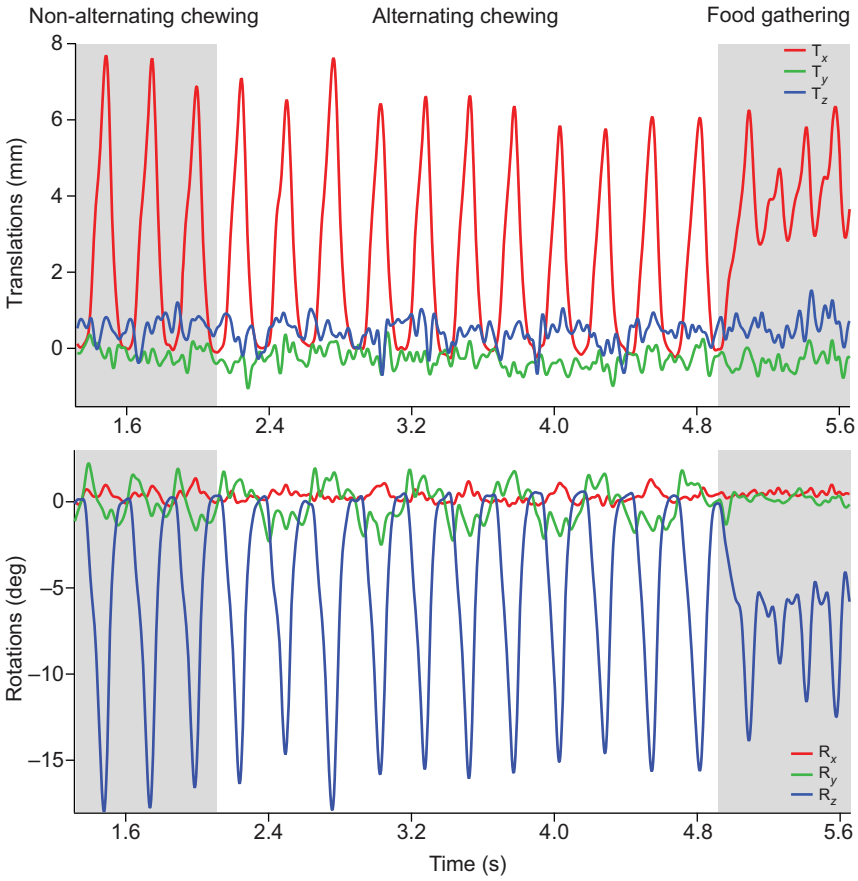

Fig. 3. A representative feeding sequence from Sus A, illustrating the feeding behaviors observed in this study. This sequence starts with three non-alternating right-side chews. Note the increasing R_y, indicating yaw toward the left (balancing side) during the first three occlusions. The non-alternating chews are followed by a series of 11 alternating cycles that begins and ends with left-sided chews, and finally finishes with four cycles of food gathering.

capacity to measure such movements with high precision. These attributes made it possible for us to quantify both the direction and the magnitude of exact movements, such as the premolar displacements that occur during the power stroke of occlusion. In using XROMM we also were able to integrate rigid body movements of the mandible with displacements of anatomical landmarks. This allowed us to explore the dental movements of mastication in the context of mandibular translations and rotations around a more posterior joint. XROMM thus represents an opportunity to precisely quantify both dental and skeletal motions that are externally observable (e.g. gape, incisor displacements) (Brainerd et al., 2010), as well as motions that have traditionally been obscured by soft tissues (e.g. post-canine occlusion, TMJ displacements).

Furthermore, through XROMM we also were able to document the absence of certain mandibular motions during feeding. We determined precision thresholds for the kinematic variables in this study (see 'Precision study' in Materials and methods). These thresholds allowed us to distinguish measurable, repeatable motions from any noise introduced in the XROMM workflow. In this study, we were able to quantify mandibular movements to within 0.50 mm for rigid body translations and 3D anatomical landmark displacements, and within 0.25 deg for rigid body rotations. While the pig mandible can potentially move within six degrees of freedom, we recorded mandibular movements during mastication along only three of the six possible axes: translations along a propalinal axis, and rotations around dorsoventral (yaw) and transverse (pitch) axes. We did not detect repeatable motions in the remaining three degrees of freedom: translations along dorsoventral and mediolateral axes, and rotations around an anteroposterior axis (roll).

Movements in these three unoccupied degrees of freedom might have been reasonably expected, but were not reliably observed within the precision limits of this study. First, translation of the jaw along a dorsoventral axis was not detected within a 0.26 mm precision threshold. Dorsal translation of the jaw might accompany compression of the TMJ during the closing and occlusal phases of chewing, but this was observed only in a single individual, Sus D (supplementary material Fig. S1). This individual also displayed the most conservative chews, with restricted magnitudes of jaw protraction and depression (Fig. 7). These kinematic differences may be related to the pathology of the jaw joint in Sus D, such as a displaced TMJ disc. Second, translation of the mandible along a mediolateral axis was not detected within a 0.44 mm precision threshold. In human dentistry, the WS condyle is thought to translate laterally along the lateral incline of the mandibular fossa during jaw opening. This motion, known as 'Bennett movement', occurs at magnitudes of about 1–3 mm (Bennett, 1908; Peck, 1988). However, we did not observe lateral translations of the mandible or the condyle during mastication in miniature pigs. Our results are consistent with the view that Bennett movements are not true translations, but rather protrusions of the lateral pole of the WS condyle produced by condylar rotation as the opening jaw yaws towards the WS (Landa, 1958a,b). The combination of a well-developed medial capsular ligament and the lateral zygomatic flange may also limit lateral translations of the mandibular condyle in pigs as compared with humans (Herring et al., 2002; Sun et al., 2002). Third, and finally, rotation of the jaw about an anteroposterior axis (roll) was not detected within a 0.26 deg precision threshold. Species with unfused mandibular symphyses may experience independent roll rotations of the hemimandibles during feeding. However, in taxa with fused symphyses (e.g. the

The Journal of Experimental Biology (2015) 218, 2573-2584 doi:10.1242/jeb.119438

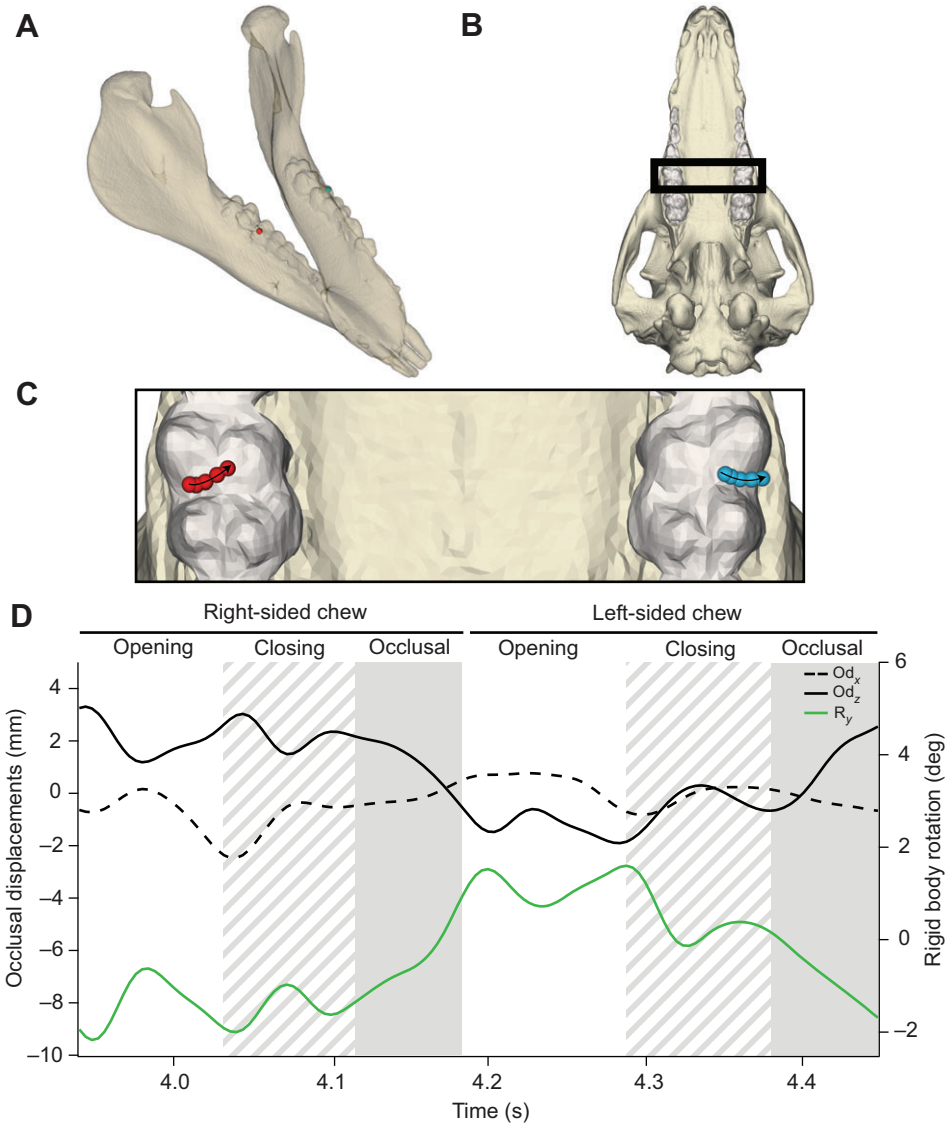

Fig. 4. Displacements of the mandibular premolars (dP4) during occlusion. (A) Spheres were fitted to the distobuccal cusp of the dP4s (right, red; left, blue) in Sus D. (B) An inferior view of the cranium; the boxed area is magnified in C. (C) Time-lapse traces (five overlapping spheres) of displacements of the mandibular dP4 cusps/spheres (right, red; left, blue) shown against the opposing maxillary dP4s during the occlusal phase of a right-sided chew. (D) A representative trace of occlusal displacements (right dP4) and mandibular rigid body yaw during an alternating chewing cycle in Sus A. During occlusion, the mandible yaws towards the balancing side (R_y), which produces both the buccolingual (Od_z) and mesiodistal (Od_x) occlusal movements of the teeth during the power stroke. See Table 5 for mean occlusal displacements among individuals.

pig), mandibular roll toward the WS could compromise the masticatory system by increasing tension at the WS TMJ and causing joint distraction (Greaves, 1978; Lieberman and Crompton, 2000; Wright, 2005). If motions in these three unoccupied degrees of freedom exist during mastication, they occur at magnitudes below the precision threshold specific to that kinematic variable.

Table 5. Occlusal displacement measurements of the right mandibular dP4

	Right-sided chew (ipsilateral)		Left-sided chew (contralateral)	
	ΔOd_x	ΔOd_z	ΔOd_x	ΔOd_z
Sus A	1.00	–2.68	–0.84	2.84
(*N*=5 chews)	(0.28)	(0.59)	(0.16)	(0.25)
Sus B	0.54	–1.58	–0.40	1.79
(*N*=4 chews)	(0.35)	(0.90)	(0.10)	(0.65)
Sus D	0.58	–1.83	–0.41	1.74
(*N*=7 chews)	(0.49)	(1.08)	(0.11)	(0.54)

Displacement measurements (mm) are means (s.d.) and are shown as values relative to the ACS.
Directionality key: ΔOd_x, posterior displacement≤0≥anterior displacement; ΔOd_z, left-wards displacement≤0≥right-wards displacement.

Mandibular movements were even more restricted in other feeding behaviors, such as food gathering and nut cracking, where we observed movements only in two degrees of freedom (propalinal translation and pitch rotations). These negative results underscore the importance of defining precision thresholds for XROMM studies, in order to place limits on what can be realistically interpreted as motion within a given workflow.

Although conferring many advantages, the XROMM technique is not ideal for answering all questions about jaw movement during mastication. As it is essential to be able to visualize the radiopaque markers, the bolus could not be labeled, and therefore it remains unknown whether bolus size or position influences the chewing stroke. In addition, it is not feasible to capture and analyze full feeding sequences, which may include as many as 60 individual cycles in miniature pigs (Herring and Scapino, 1973); thus, we could not evaluate the importance of intra-sequence cycle variation.

Concluding remarks

Pigs are a common model organism for studying human masticatory function, because of the omnivore status of pigs and the similarities in TMJ morphology between domestic pigs and anthropoid

The Journal of Experimental Biology (2015) 218, 2573-2584 doi:10.1242/jeb.119438

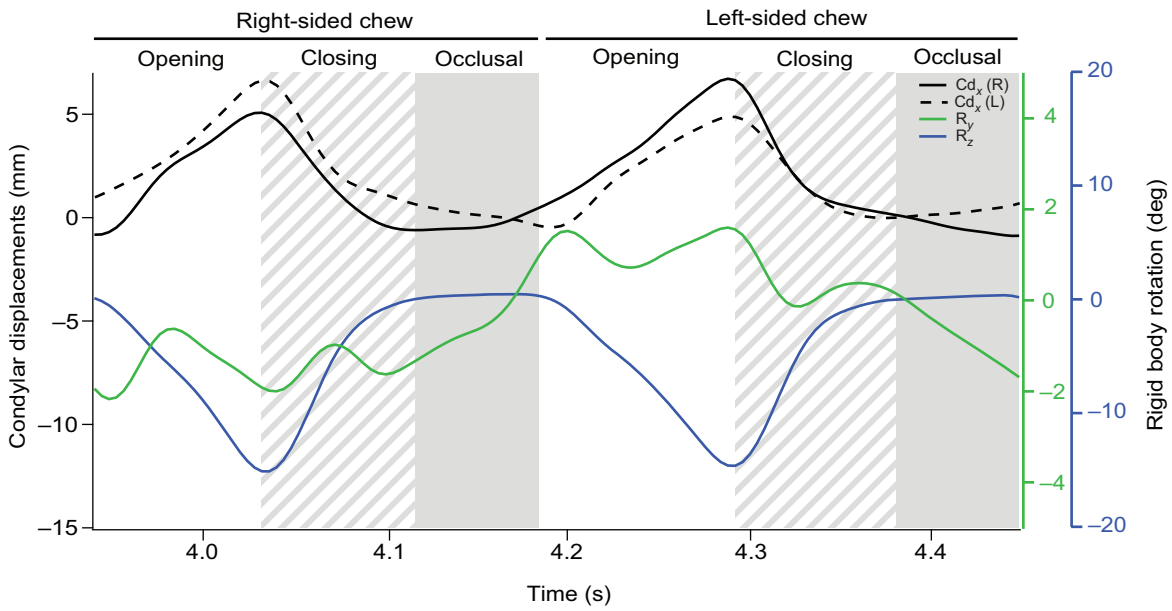

Fig. 5. Representative trace of anteroposterior condylar displacements and mandibular rigid body rotations during an alternating chewing cycle in Sus A. Displacements of the right (solid) and left (dotted) mandibular condyles are shown. Anteroposterior displacements of the mandibular condyle (Cd_x) are primarily produced by mandibular pitch (R_z), but the magnitude of these displacements is greater during contralateral chews [balancing side (BS) condylar function] as a result of mandibular yaw (R_y). During occlusion in the right-sided chew, the contralateral/BS (left) condyle retracts while the ipsilateral/WS (right) condyle protracts slightly. This asymmetry of condylar motions is associated with yaw (increasing R_y) of the mandible toward the left (BS).

primates (Herring, 2003). Indeed, the generalized nature of the pig masticatory apparatus makes this species – and this study – well placed as an initial foray into XROMM analyses of mammalian mastication. Here, we were able to test how hypothetical kinematics inferred from tooth (e.g. transverse enamel ridges) and TMJ structure compared with the actual kinematics observed during naturalistic feeding behaviors. Notably, soft tissue structures such as joint capsule ligaments appear to play a significant role in limiting the range of motion of a joint. Analyses based on osseous structures alone, as is often necessary in fossil specimens, may thus be susceptible to over-estimating joint mobility.

Comparative studies are needed to understand whether feeding behaviors in non-omnivore species are characterized by kinematic flexibility (e.g. jaw posture flexibility), as they are in the miniature pig. Comparative studies are also needed to determine the extent to which other mammalian taxa may use jaw movements in degrees of freedom that were not noted in the miniature pig. Future XROMM studies of taxa with more specialized masticatory apparatuses, such as carnivores or ruminant artiodactyls, are necessary to further elucidate the association between craniomandibular morphology and feeding kinematics.

MATERIALS AND METHODS

This study describes the feeding kinematics of three juvenile (4 month old) Hanford strain miniature pigs (*S. scrofa*), referred to as Sus A, B and D. The raw data for this study were collected in 2006–2007 and used for XROMM methods development (Brainerd et al., 2010), but a full analysis of feeding kinematics in these pigs has not previously been published. Procedures for the surgical implantation of radiopaque markers, biplanar videofluoroscopy, and CT scanning and creation of polygonal mesh models are described in detail in Brainerd et al. (2010). During feeding trials used to describe chewing and food-gathering kinematics, pigs were fed a standard pellet diet. Two individuals (Sus A and D) were fed unshelled walnuts or brazil nuts in separate trials in order to compare the crushing behavior associated with hard food items with the mastication of pellets. All procedures and animal care were approved by the Brown University Institutional Animal Care and Use Committee (protocol 33-07).

Dental anatomy

In juvenile Hanford miniature pigs, the dental formula is 3.1.4/3.1.4 (deciduous incisors, canines and premolars); in adults, it is 3.1.4.3/3.1.4.3 (permanent incisors, canines, premolars and molars). Mastication in juveniles thus occurs along a relatively short row of deciduous premolars until the eruption of the first permanent molar, which takes place after 4 months of age in miniature breeds (Weaver et al., 1969; Huang et al.,

Table 6. Condylar retraction measurements during the closing and occlusal phases of ipsilateral chews (WS function) and contralateral chews (BS function)

	Closing phase			Occlusal phase		
	ΔCd_x WS	ΔCd_x BS	*P*-value	ΔCd_x WS	ΔCd_x BS	*P*-value
Sus A	5.92	6.34	0.50	−0.66	1.09	**0.00**
(*N*=9 chews)	(0.85)	(1.04)		(0.13)	(0.52)	
Sus B	4.33	5.08	0.12	−0.15	0.90	**0.01**
(*N*=9 chews)	(1.97)	(2.44)		(0.86)	(0.86)	
Sus D	3.56	4.55	**0.00**	−0.39	0.69	**0.00**
(*N*=14 chews)	(0.45)	(0.44)		(0.39)	(0.24)	

Retraction measurements (mm) are means (s.d.) and are for pooled left and right condylar movements. Positive mean values indicate retraction, negative mean values indicate protraction. WS, working side; BS, balancing side.
P-values in bold are significant.

The Journal of Experimental Biology (2015) 218, 2573-2584 doi:10.1242/jeb.119438

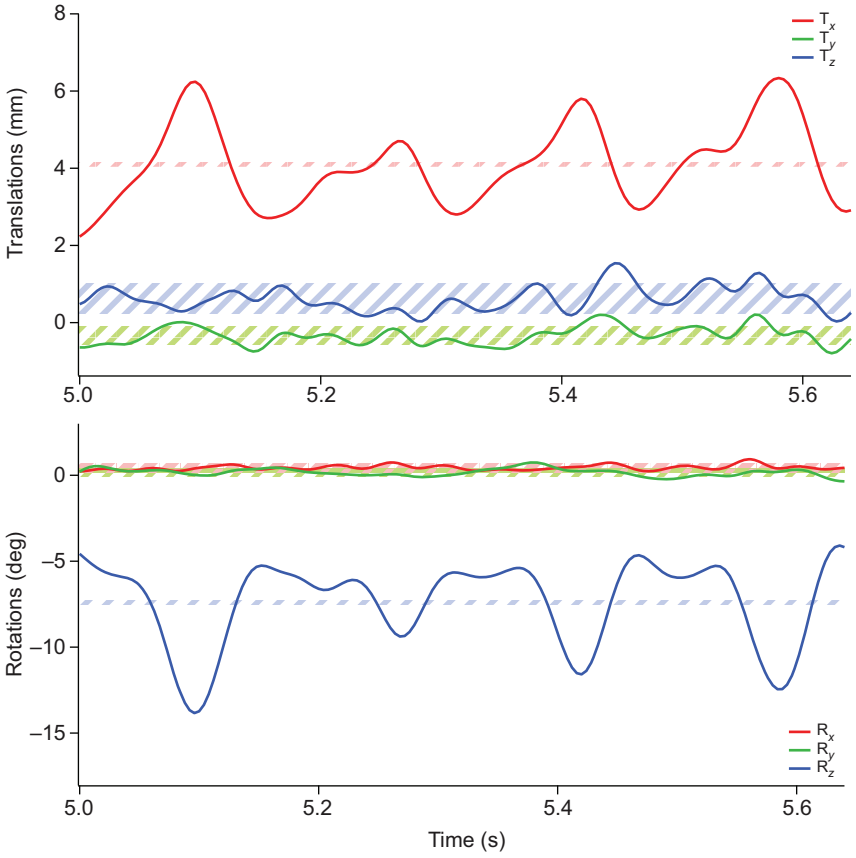

Fig. 6. Representative sequence of mandibular kinematics during food gathering from Sus A. Hatched bars show the precision thresholds for the six-degree-of-freedom traces. Tongue and food motions could not be seen consistently in all X-ray videos, but it was clear that, during pellet food gathering, the tongue protracts when the mandible depresses (decreasing R_z), food collects on the surface of the tongue, and then the tongue retracts as the mandible elevates.

1994). In the pigs used in this study, the first permanent molar had erupted but was not yet in occlusion. Minimal wear was present on the erupted deciduous teeth. The mesial deciduous premolars (maxillary dP1–2, mandibular dP1–3) were small and unmolarized in their morphology. Maxillary dP3–4 and mandibular dP4 were molariform with bunodont occlusal surfaces, and thus were the focus of this study.

XROMM analysis

X-ray videos were analyzed using the XrayProject program in Matlab (R2013b, The MathWorks, Natick, MA, USA), which is described in detail and available at xromm.org. Standard grid images were used to correct for distortion of the videos introduced by the X-ray machine image intensifiers. Images of a calibration object with known geometry (a cube with 64 radiopaque markers) were used to calibrate the 3D space.

The precision of XROMM marker tracking can be calculated as the standard deviation of the mean distance between markers within a single bone during the motion sequence (Brainerd et al., 2010). Collating inter-marker distance standard deviations for 9–10 markers per trial, 3–6 trials per individual, and 3 individuals, mean marker tracking precision for this study was 0.11 mm (N=51 pairwise inter-marker distances).

Marker coordinates (x,y,z) were filtered using a low-pass Butterworth filter with 25 Hz cutoff frequency. Filtered marker coordinates were then used to calculate rigid-body translations and rotations of the cranium and mandible (Brainerd et al., 2010). Animations were produced by applying rigid body transformations to the polygonal mesh bone models in Autodesk Maya (2013, Autodesk Inc., San Rafael, CA, USA).

Joint and anatomical coordinate systems

To describe the 3D movement of the mandible relative to the cranium, a JCS was created in Autodesk Maya (Brainerd et al., 2010) (Figs 1, 2). A JCS measures the three ordered rotations and three translations of an ACS attached to a distal bone (e.g. mandible) relative to an ACS attached to a proximal bone (e.g. cranium). For each individual, a neutral posture was chosen where the maxillary and mandibular incisors were in centric occlusion. An ACS was then created for the mandible in this neutral posture by creating and aligning a plane parallel to the occlusal surfaces of the post-canine teeth (Fig. 1A). This plane was then translated dorsally to intersect a z-axis passing through the medial-most point of both mandibular condyles. The x-axis was aligned along the occlusal plane, centering the ACS between the condyles, and the y-axis was set orthogonal to the z- and x-axes. A second ACS was then created with the same location and orientation as the mandibular ACS in its zero position (neutral posture). This second ACS was parented to the cranium to become the proximal ACS for describing relative movement of the distal mandibular ACS. Kinematic variables (translations and rotations) extracted from the JCS are described in Table 1.

3D displacements of anatomical landmarks were measured relative to the cranial ACS described above (Fig. 1B,C). Locators were created in Maya and then snapped to the surface of the mesh model at the anatomical location of interest (Fig. 1B). One locator was attached to the distobuccal cusp of the right mandibular deciduous fourth premolar (dP4). Locators were also attached to the medial-most point of the mandibular condyles, both left and right. Kinematic variables (displacements) for these locators measured relative to the ACS are described in Table 1.

Data analysis

Kinematic data were analyzed to describe mandibular motion and anatomical locator displacements during mastication and food gathering. Changes in jaw retraction (ΔT_x) and jaw closing (ΔR_z) within a single chew or food-gathering movement were quantified for the mandibular rigid body (Table 2). During mastication, maximum jaw protrusion and depression occur in the opening phase, and maximum jaw retrusion and elevation occur in the occlusal phase. During food gathering, measurements were taken from the semi-cyclical movements that are observed during this behavior (see Fig. 3).

The amount of jaw protraction ($+T_x$, mm) produced by a degree of jaw depression ($-R_z$, deg) during the opening phase of a chew was quantified for each individual. This value was calculated as the absolute value of the slope from a least squares regression of opening-phase T_x values against R_z values.

The Journal of Experimental Biology (2015) 218, 2573-2584 doi:10.1242/jeb.119438

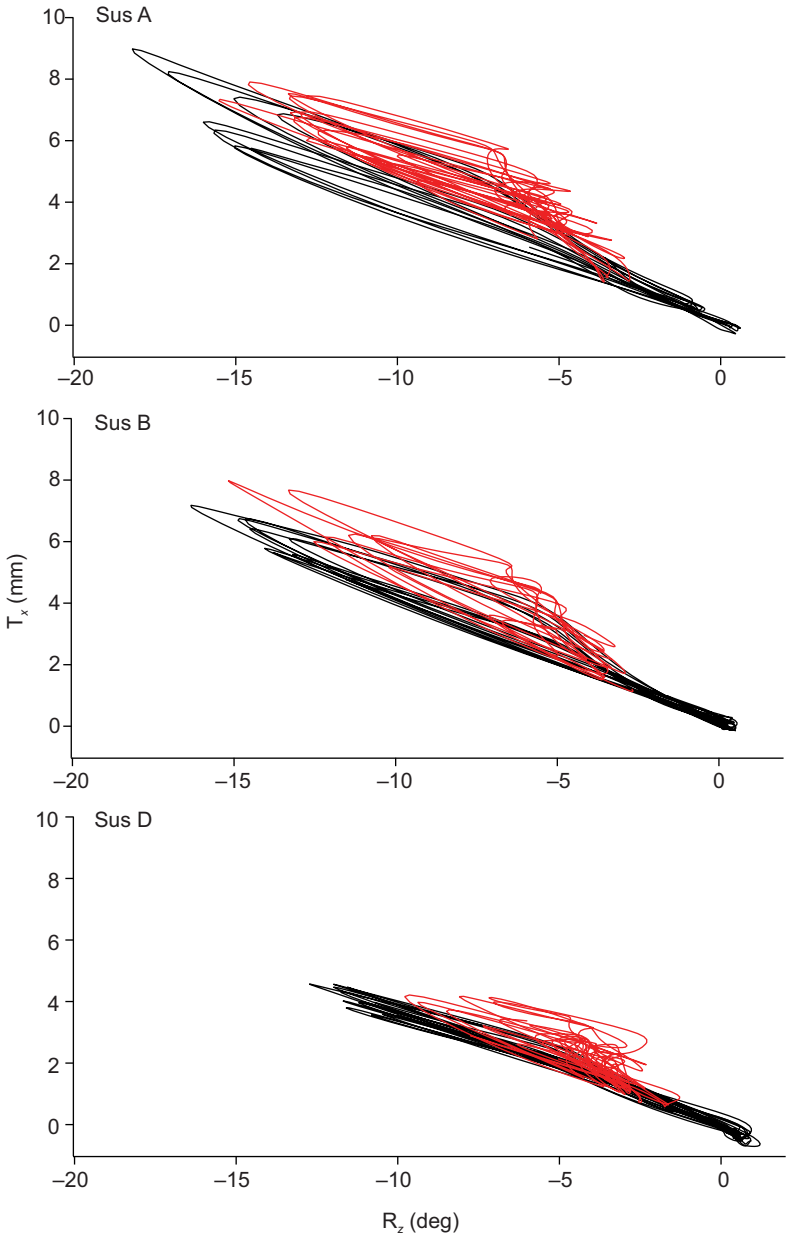

Fig. 7. Mandibular propalinal translation (T_x) relative to depression–elevation (R_z) during mastication and food gathering. The mandible is held in a protracted posture during food gathering (red) when compared with chewing (black), and jaw opening and closing occurs in a reduced range during food gathering.

Changes (Δ) in anatomical locator displacements were also quantified (Table 2). For the locator attached to the right mandibular dP4, changes in displacements along mesiodistal and buccolingual axes, ΔOd_x and ΔOd_z, respectively, were quantified during the occlusal phase. For the locators attached to the mandibular condyles, changes in jaw retraction (ΔCd_x) were measured between maximum jaw protrusion during the opening phase and maximum jaw retrusion during the occlusal phase.

Animated polygonal mesh bone models for Sus D were used to visualize the displacements of the right mandibular dP4 locator during occlusion. First, a sphere was fitted to the distobuccal cusp of the tooth, interior to the location of the locator, in Maya. Then, a time-lapse trace of the path of this sphere was created using the Animation Snapshot tool. The snapshot captured increments of 0.016 s between 4.57 and 4.62 s, the duration of the occlusal phase during a single right-sided chew.

Condylar retraction (ΔCd_x) was measured for both left and right mandibular condyles during both right- and left-sided chews. Retraction measurements were taken during the chewing and occlusal phases of each chew. Measurements taken from the left and right condyles were pooled together by WS and BS function, as no statistical difference existed between the left and right condyles in these measurements. A statistical comparison of pooled WS versus BS function condylar retraction measures was performed using a Kruskal–Wallis analysis (α=0.05).

Precision study

A study was conducted to assess the precision of the XROMM workflow specific to this study. Following the completion of the *in vivo* study, Sus B was euthanized and its skull collected and frozen. The cadaveric skull was then substituted for a live subject in the XROMM workflow. Joints in a frozen specimen should be immobile, and thus all relative motions between markers and bones should be zero. The amount of deviation from zero is the measurement of precision for this study. Precision measurements were then applied to *in vivo* data as a determination of the magnitude of movements necessary to confidently interpret such movements as real motion versus noise from imprecision in the workflow.

The cadaveric skull was suspended in the biplanar x-ray field of view and moved with a radiopaque wooden pole at a frequency similar to that of head movement during feeding. Videos from the fluoroscopes were collected at 250 frames s^{-1}, 80–83 kV and 12.0–12.5 mA.

X-ray videos were undistorted, 3D space was calibrated, and markers were digitized and filtered as described above (see XROMM analysis).

The Journal of Experimental Biology (2015) 218, 2573-2584 doi:10.1242/jeb.119438

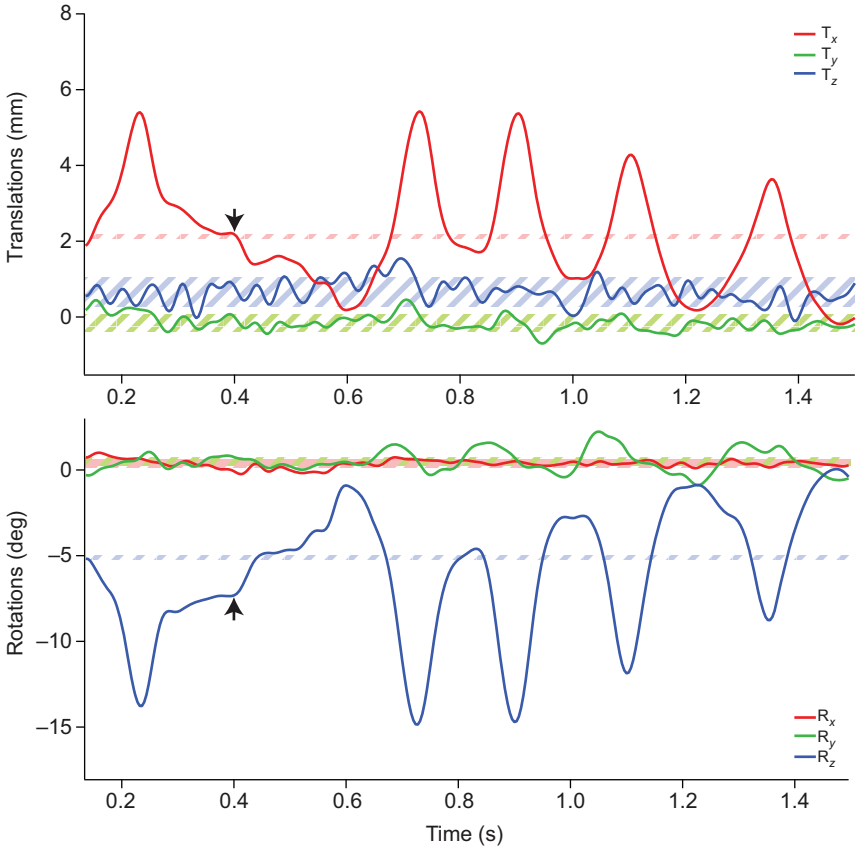

Fig. 8. Representative sequence of nut crushing and processing from Sus A. Hatched bars show the precision thresholds for degree-of-freedom traces. An arrow indicates the timing of the nut crack.

Collating the inter-marker distance standard deviations for nine markers and two trials, the mean s.d. was ±0.15 mm (N=36 pairwise inter-marker distances). Rigid body kinematics were calculated from digitized marker x,y,z coordinates and used to animate bone movements.

Similar to the *in vivo* analyses, kinematic variable data were collected relative to the JCS and ACS (Table 1). Standard deviations were calculated for each kinematic variable as a measure of workflow precision (Table 3). Precision thresholds for *in vivo* data were then calculated as the mean of the kinematic variable within the video frames of interest ±the precision value (standard deviation) for that variable. For example, in Fig. 2, the mean of T_x between 3.9 and 4.4 s is 1.80 mm, and the precision threshold for T_x in these frames is 1.80±0.06 mm (Fig. 2, Table 3). Where kinematic variables failed to exceed their precision threshold, they were considered to be noise from imprecision that accumulated during the XROMM workflow. Only when kinematic variables exceeded the precision threshold could they be confidently interpreted as real *in vivo* movements. The precision values reported here are specific to this study. Higher precision can be achieved for smaller animals by using a smaller X-ray field of view, and with improvements in marker-tracking and filtering software.

Acknowledgements

We thank J. Bahlman, A. Clifford, N. Gidmark and B. Nowroozi for assistance with pig training, A. Clifford for assistance with surgeries, C. Crynes, M. Dawson, S. Geoghegan, C. Harper, A. Lin and A. Sullivan for data analysis, and E. Tavares and A. Sullivan for outstanding technical and administrative assistance.

Competing interests

The authors declare no competing or financial interests.

Author contributions

K.A.M., E.L.B. and S.W.H. conceived and designed the study, K.A.M. developed the surgical techniques and performed the surgeries, K.A.M., E.L.B. and D.B.B. collected the data, K.A.M., E.L.B., D.B.B. and R.A.M. analyzed the data, R.A.M., S.W.H. and E.L.B. developed the tooth occlusion and TMJ analyses, R.A.M. made the figures and wrote the manuscript, and all authors reviewed, edited and approved the manuscript.

Funding

This work was supported by the Bushnell Graduate Education and Research Fund, the W. M. Keck Foundation, and the US National Science Foundation [grant numbers 0552051, 0840950, 1262156 to E.L.B. and grant numbers 1262124 and 1004057 to D.B.B.].

Supplementary material

Supplementary material available online at
http://jeb.biologists.org/lookup/suppl/doi:10.1242/jeb.119438/-/DC1

References

Bennett, N. G. (1908). A contribution to the study of the movements of the mandible. *Proc. R. Soc. Med.* **1**, 79-98.

Bodegom, J. C. (1969). *Experiments on Tooth Eruption in Miniature Pigs*. Nijmegen, The Netherlands: Gebr. Janssen.

Brainerd, E. L., Baier, D. B., Gatesy, S. M., Hedrick, T. L., Metzger, K. A., Gilbert, S. L. and Crisco, J. J. (2010). X-ray reconstruction of moving morphology (XROMM): precision, accuracy and applications in comparative biomechanics research. *J. Exp. Zool. A* **313A**, 262-279.

Graves, H. B. (1984). Behavior and ecology of wild and feral swine (*Sus scrofa*). *J. Anim. Sci.* **58**, 482-492.

Greaves, W. S. (1978). The jaw lever system in ungulates: a new model. *J. Zool.* **184**, 271-285.

Hatley, T. and Kappelman, J. (1980). Bears, pigs, and Plio-Pleistocene hominids: a case for the exploitation of belowground food resources. *Hum. Ecol.* **8**, 371-387.

Herring, S. W. (1976). The dynamics of mastication in pigs. *Arch. Oral Biol.* **21**, 473-480.

Herring, S. W. (1985). Morphological correlates of masticatory patterns in peccaries and pigs. *J. Mammal.* **66**, 603-617.

Herring, S. W. (1993). Functional morphology of mammalian mastication. *Am. Zool.* **33**, 289-299.

Herring, S. W. (2003). TMJ anatomy and animal models. *J. Musculoskelet. Neuronal Interact.* **3**, 391-394.

Herring, S. W. and Scapino, R. P. (1973). Physiology of feeding in miniature pigs. *J. Morphol.* **141**, 427-460.

Herring, S. W., Rafferty, K. L., Liu, Z. J. and Marshall, C. D. (2001). Jaw muscles and the skull in mammals: the biomechanics of mastication. *Comp. Biochem. Physiol. A Mol. Integr. Physiol.* **131**, 207-219.

Herring, S. W., Decker, J. D., Liu, Z.-J. and Ma, T. (2002). Temporomandibular joint in miniature pigs: anatomy, cell replication, and relation to loading. *Anat. Rec.* **266**, 152-166.
Huang, X., Zhang, G. and Herring, S. W. (1994). Age changes in mastication in the pig. *Comp. Biochem. Physiol. A Physiol.* **107**, 647-654.
Hylander, W. L., Wall, C. E., Vinyard, C. J., Ross, C., Ravosa, M. R., Williams, S. H. and Johnson, K. R. (2005). Temporalis function in anthropoids and strepsirrhines: an EMG Study. *Am. J. Phys. Anthropol.* **128**, 35-56.
Janis, C. M. and Fortelius, M. (1988). On the means whereby mammals achieve increased functional durability of their dentitions, with special reference to limiting factors. *Biol. Rev. Camb. Philos. Soc.* **63**, 197-230.
Landa, J. S. (1958a). A critical analysis of the Bennett movement. Part I. *J. Prosthet. Dent.* **8**, 709-726.
Landa, J. S. (1958b). A critical analysis of the Bennett movement. Part II. *J. Prosthet. Dent.* **8**, 865-879.
Langenbach, G. E. J., Zhang, F., Herring, S. W. and Hannam, A. G. (2002). Modelling the masticatory biomechanics of a pig. *J. Anat.* **201**, 383-393.
Lieberman, D. E. and Crompton, A. W. (2000). Why fuse the mandibular symphysis? A comparative analysis. *Am. J. Phys. Anthropol.* **112**, 517-540.
Liu, Z. J. and Herring, S. W. (2001). Masticatory strains on osseous and ligamentous components of the temporomandibular joint in miniature pigs. *J. Orofac. Pain* **14**, 265-278.
Obrez, A. (1996). Mandibular molar teeth and the development of mastication in the miniature pig (*Sus scrofa*). *Acta Anat.* **156**, 99-111.
Peck, C. C. (1988). An assessment of condylar kinematics. MS Thesis, University of Sydney.
Scheman, P. (1967). Anthropoid comparisons of the anatomy of the external pterygoid muscles of the fetal and adult domestic pig. *J. Dent. Res.* **46**, 1337-1343.
Sindelar, B. J. and Herring, S. W. (2005). Soft tissue mechanics of the temporomandibular joint. *Cells Tissues Organs* **180**, 36-43.
Smith, J. M. and Savage, R. J. G. (1959). The mechanics of mammalian jaws. *Sch. Sci. Rev.* **40**, 289-301.
Sun, Z., Liu, Z.-J. and Herring, S. W. (2002). Movement of temporomandibular joint tissues during mastication and passive manipulation in miniature pigs. *Arch. Oral Biol.* **47**, 293-305.
Taylor, R. B. (1999). Seasonal diets and food habits of feral swine. In *Proceedings of the First National Feral Swine Conference*, pp. 58-66. Ft Worth, Texas: Texas Animal Health Commission.
Weaver, M. E., Jump, E. B. and McKean, C. F. (1969). The eruption pattern of permanent teeth in miniature swine. *Arch. Oral Biol.* **14**, 323-331.
Weijs, W. A. (1994). Evolutionary approach of masticatory motor patterns in mammals. In *Biomechanics of Feeding in Vertebrates*, Vol. 18 (ed. V. Bels, M. Chardon and P. Vandewalle), pp. 281-320. Berlin, Heidelberg: Springer.
Williams, S. H., Vinyard, C. J., Wall, C. E. and Hylander, W. L. (2007). Masticatory motor patterns in ungulates: a quantitative assessment of jaw-muscle coordination in goats, alpacas and horses. *J. Exp. Zool. A Ecol. Genet. Physiol.* **307A**, 226-240.
Wright, B. W. (2005). Craniodental biomechanics and dietary toughness in the genus Cebus. *J. Hum. Evol.* **48**, 473-492.

The Journal of Experimental Biology